

Evidence for UHECR origin in starburst galaxies

Luis A. Anchordoqui

Department of Physics & Astronomy, Lehman College, CUNY, NY 10468, USA

Department of Physics, Graduate Center, City University of New York, NY 10016, USA

Department of Astrophysics, American Museum of Natural History, NY 10024, USA

E-mail: luis.anchordoqui@gmail.com

Jorge F. Soriano*

Department of Physics & Astronomy, Lehman College, CUNY, NY 10468, USA

Department of Physics, Graduate Center, City University of New York, NY 10016, USA

E-mail: jfdezsoriano@gmail.com

The quest for the origin(s) of ultra-high-energy cosmic rays (UHECRs) continues to be a far-reaching pillar of high energy astrophysics. The source scrutiny is mostly based on three observables: the energy spectrum, the nuclear composition, and the distribution of arrival directions. We show that each of these three observables can be well reproduced with UHECRs originating in starburst galaxies.

*36th International Cosmic Ray Conference - ICRC2019 -
July 24 - August 1, 2019
Madison, Wisconsin, USA*

*Speaker.

Starburst galaxies are observed to be forming stars at an unusually fast rate (about 10^3 times greater than in a normal galaxy). The areas of high activity can be spread throughout the galaxy, but most star forming regions are observed in a small sector around the nucleus. The starburst activity usually drives galactic-scale outflows or “superwinds” that may be responsible for removing metals from the galactic disk and polluting the intergalactic medium with ultra-high-energy ($E \gtrsim 10^9$ GeV) cosmic ray (UHECR) nuclei [1–4]. Starburst superwinds are powered by massive star winds and by core collapse supernovae which collectively create hot ($T \lesssim 10^8$ K) bubbles of metal-enriched plasma within the star forming regions [5]. The over-pressured bubbles expand, sweep up cooler ambient gas, and eventually blow out of the disk into the halo, providing a profitable arena for the formation of collisionless plasma shock waves, in which UHECRs can be accelerated by bouncing back and forth across the shock. Herein we present additional support for this idea by confronting the predictions of the model with experimental data.

Specific assumptions are made, in that we consider diffusive shock acceleration on a distribution of particles at multiple parallel shocks (in which both the magnetic field and the upstream and downstream plasma flows are always perpendicular to the plane of the shock front).¹ Note since the magnetic field has components only along the direction in which the shock propagates the Rankine-Hugoniot jump conditions are hydrodynamic in character (see Appendix). At each shock a new distribution of particles is injected and accelerated, and the particles injected at earlier shocks are re-accelerated further. Adiabatic decompression occurs after each shock. We show that these considerations reduce the time constraint on the acceleration region, while addressing the criticism on the model raised in [7]. Moreover, the presence in the wind of many shocks changes the particle spectrum from that produced by a single shock [8]. Summing over an infinite number of identical shocks, with fresh injection at each shock and decompression between the shocks, does produce a power-law momentum distribution $f_\infty(p) \propto p^{-3}$ [9], which is flatter than that produce by a single shock $f(p) \propto p^{-4}$, and better reproduce observations.

The UHECR spectrum can be roughly described by a twice-broken power law [10–13]. The first break is a hardening of the spectrum, known as “the ankle.” The second is an abrupt softening of the spectrum, which (i) may be interpreted as the long-sought GZK cutoff [14,15], or (ii) may correspond to the “end-of-steam” for cosmic accelerators [16,17]. Herein we introduce a complementary explanation (iii) in which GZK interactions at the source constrain the maximum energy of the nuclei. Note that (iii) is markedly different from (ii) because for a nucleus of charge Ze and baryon number A , the maximum energy of acceleration capability of the sources grows linearly in Z , while the energy loss per distance traveled decreases with increasing A . The ankle energy and the corresponding change in the power-law spectral index are measured with high precision. The existence of the flux suppression is also firmly established. The differential energy spectra measured by the Telescope Array (TA) experiment [10,13] and the Pierre Auger Observatory (Auger) [11,12] agree within systematic errors below $E \sim 10^{10}$ GeV; at higher energies, TA observes more

¹It has long been known that stellar winds contain a network of embedded shocks [6]. This provides some support for our conjecture.

cosmic rays than would be expected if the spectral shape were the same as that seen by Auger. The flux suppression observed in Auger data is at $E \sim 10^{10.6}$ GeV, whereas the one observed in TA data is at $E \sim 10^{10.73}$ GeV.

The TA Collaboration has interpreted their data as implying a light primary composition (mainly p and He) from $10^{9.1}$ to $10^{10.6}$ GeV [18, 19]. The Auger Collaboration, using post-LHC hadronic interaction models, reports a composition becoming light up to $10^{9.3}$ GeV but then becoming heavier above that energy, with the mean mass intermediate between protons and iron at $10^{10.5}$ GeV [20–24]. Auger and TA have also conducted a thorough joint analysis and state that, at the current level of statistics and understanding of systematics, both data sets are compatible with being drawn from the same parent distribution, and that the TA data is compatible both with a protonic composition below 10^{10} GeV and with the mixed composition above 10^{10} GeV as reported by Auger [25, 26]. However, Auger data are more constraining and not compatible with the pure protonic option available with TA alone. Moreover, a recent re-analysis of TA data seems to indicate that a pure proton composition above the ankle is disfavored [27].

The high frequency spectral fall-off and the shape of the spectrum at and below the corner frequency are critical to assess the characteristics of the source spectra. In particular, a simultaneous fit to the spectrum and the elongation rate requires hard source spectra $\propto E^{-\gamma}$, with $1.0 \lesssim \gamma \lesssim 1.5$ [28, 29]. The differential energy spectrum $dN/dE \propto E^{-\gamma}$ is related to the phase space distribution in momentum space by $dN = 4\pi p^2 f_{\infty}(p) dp$, yielding good agreement with Auger data. The constraint on the source spectral index would be relaxed if the number of UHECR sources increases at low redshifts (for such an unusual redshift evolution softer source spectra with $dN = 4\pi p^2 f(p) dp$ are favored) [30].

The Auger Collaboration has found an indication of a possible correlation between UHECRs of $E > 10^{10.6}$ GeV and nearby starburst galaxies, with an *a posteriori* (post-trial) chance probability in an isotropic cosmic ray sky of 4.2×10^{-5} (4σ significance) [31]. The energy threshold of largest statistical significance coincides with the observed suppression in the spectrum, implying that when we properly account for the barriers to UHECR propagation in the form of energy loss mechanisms [14, 15] we obtain a self consistent picture for the observed UHECR horizon. The TA Collaboration has reported that with their current statistics [32] they cannot make a statistically significant corroboration or refutation of the reported possible correlation between UHECRs and starburst galaxies. However, TA has recorded a statistically significant excess in cosmic rays, with energies above $10^{10.75}$ GeV, above the isotropic background-only expectation [33, 34]. This is colloquially referred to as the “TA hot-spot.” The excess is centered at Galactic coordinates $(l, b) \simeq (177^\circ, 50^\circ)$, spanning a region of the sky with $\sim 20^\circ$ radius. The chance probability of this hot spot in an isotropic cosmic ray sky was calculated to be 3.7×10^{-4} (3.4σ significance). The possible association of the TA hot-spot with the nearby (3.4 Mpc away) starburst galaxy M82 has not gone unnoticed [35, 36].

We have seen that starburst galaxies can accommodate two of the main observables in UHECR physics: the nuclear composition and the distribution of arrival directions. We turn now to discuss the acceleration process in starburst superwinds, while exploring also whether this model can accommodate the shape of the source spectra. Before proceeding,

we pause to note that very recently it was proposed that the UHECRs producing the TA hot-spot may be protons accelerated at sources in the Virgo Cluster (e.g. M87, 17 Mpc away), which propagate towards the Earth along magnetic field filaments (of strength $\gtrsim 20$ nG) [37]. However, taking data at face value we can conclude that this proposal appears unlikely: (i) as we have discussed above, a proton-dominated composition of UHECRs is disfavored by existing observations; (ii) both the spectrum and the anisotropy observed by Auger and TA can *only* be accommodated if there is a steady source within ~ 10 Mpc to account for the flux excess [38]. The latter reinforces the idea that the dominant source of the TA hot spot is the starburst galaxy M82. Another interpretation of the Auger anisotropy hints relies on UHECR acceleration in low-luminosity gamma-ray bursts [39]. However, if this were the case, the distribution of UHECRs would be isotropic in nature [40], or else correlate with the distribution of all nearby matter as opposed to a particular class of objects. It is noteworthy that when all sources beyond 1 Mpc (i.e. effectively taking out the Local Group) from the 2MRS catalog are included as part of the anisotropic signal in the analysis of [31] the significance level reduces to 3σ . Therefore, we can conclude that the interpretation of the anisotropy signal in terms of low-luminosity gamma-ray bursts is disfavored by data.

With the motivation loaded we can now look at the calculations. The UHECR emission from starbursts is attributed to shock accelerated particles. We describe the acceleration of these particles through the energy gain $g \equiv dE/dt$. We consider acceleration at superwind-embedded shocks in which the gain g_{SW} can be described by

$$g_{\text{SW}} = \frac{\xi E}{T_{\text{cycle}}}, \quad (1)$$

where

$$T_{\text{cycle}} = 4\kappa \left(\frac{1}{u_1} + \frac{1}{u_2} \right) \quad (2)$$

is the duration of each acceleration cycle,

$$\xi \sim \frac{4}{3}(u_1 - u_2) \quad (3)$$

is the fractional energy gain per encounter,

$$\kappa = \frac{1}{3}R_L \sim \frac{1}{3} \frac{E}{ZeB} \quad (4)$$

is the diffusion coefficient, R_L is the Larmor radius, and u_1 and u_2 are the upstream and downstream gas velocities [41, 42]. For simplicity, we demand that any two shocks do not propagate simultaneously. Studies of more general set-ups, with shock correlation effects, are underway and will be presented elsewhere [43]. For typical superwind parameters $u_2 = u_1/4$ and $u \equiv u_1 \sim 1.8 \times 10^3$ km/s, the energy gain

$$g_{\text{SW}}^{(Z)}(B) = \frac{3}{20} ZeBu^2, \quad (5)$$

produces a linear increase of energy as a function of time

$$\mathcal{E}(E_0, t_0, t) = E_0 + g_{\text{SW}}^{(Z)}(t - t_0), \quad (6)$$

for a fixed magnetic field.² Thus, for an accelerator of size $R_{\text{SW}} \sim 8$ kpc, the maximum energy is

$$E_{\text{max}} \sim g_{\text{SW}}^{(Z)} \Delta t, \quad (7)$$

where $\Delta t = t - t_0$. For a single shock, we have $\Delta t = R_{\text{SW}}/u$. Substituting this relation into (7) leads to the Hillas maximum rigidity [46]

$$\mathcal{R}_{\text{H,max}} \sim 10^9 (u/c) \left(\frac{B}{\mu\text{G}} \right) \left(\frac{R_{\text{SW}}}{\text{kpc}} \right) \text{GV}. \quad (8)$$

To develop some sense of the orders of magnitude involved, we assume that M82 and NGC 253 typify the nearby starburst population. The magnetic field B carries with it an energy density $B^2/(8\pi)$, and the flow carries with it an energy flux $> uB^2/(8\pi)$. This sets a lower limit on the rate at which the energy is carried by the out-flowing plasma,

$$L_B \sim \frac{1}{8} u R_{\text{SW}}^2 B^2, \quad (9)$$

and which must be provided by the source. The flux carried by the outgoing plasma is a model dependent parameter, which can be characterized within an order of magnitude. More concretely, $0.035 \lesssim L_B/L_{\text{IR}} \lesssim 0.35$, where $L_{\text{IR}} \sim 10^{43.9}$ erg/s is the infrared luminosity [47]. The lower limit of L_B corresponds to the estimate in [47] considering a supernova rate of 0.07 yr^{-1} , whereas the upper limit concurs with the estimate in [48], and could be obtained considering a supernova rate of 0.3 yr^{-1} [49] while pushing other model parameters to the most optimistic values. The relation (9) yields a magnetic field strength in the range

$$15 \lesssim B/\mu\text{G} \lesssim 150. \quad (10)$$

Radio continuum and polarization observations of M82 provide an estimate of the magnetic field strength in the core region of $98 \mu\text{G}$ and in the halo of $24 \mu\text{G}$; see e.g. the equipartition B map in Fig. 16 of [50]. Averaging the magnetic field strength over the whole galaxy results in a mean equipartition field strength of $35 \mu\text{G}$. Independent magnetic field estimates from polarized intensities and rotation measures yield similar strengths [51]. Comparable field strengths have been estimated for NGC 253 [52–55] and other starbursts [56]. Actually, the field strengths could be higher if the cosmic rays are not in equipartition with the magnetic field [57]. In particular, mG magnetic field strengths have been predicted [58] and measured [59] in the starburst core of Arp 220. The cosmic ray population in the starburst is dominated by the nearest accelerators in time/space to the position of interest, thus breaking a direct relation between average fields and mean cosmic ray population [60]. Up to mG field strengths are consistent with the gamma-ray and radio spectra in the gas-rich starburst cores of NGC 253 and M82 [61]. Besides, the field strength in the halo of M82 and NGC 253 could be as high as $300 \mu\text{G}$ [62–64]. In our calculations we adopt the range given in (10).

²The inferred value of u from cold and warm molecular and atomic gas observations is smaller than our fiducial value [44]. However, it is important to stress that the emission from the molecular and atomic gas most likely traces the interaction of the superwind with detached relatively denser ambient gas clouds [5], and as such it is not the best gauge to characterize the overall properties of the superwind plasma [45].

Substitution of (10) into (8) leads to $10^{8.9} \lesssim \mathcal{R}_{H,\max}/\text{GV} \lesssim 10^{9.9}$. Taking this at face value, one would tend to interpret that starburst superwinds *struggle* to accelerate light nuclei ($Z \lesssim 8$) up to the highest observed energies [7]. Note, however, that in the case of multiple shocks the time scale Δt is not constrained by the ratio of the size of the accelerator to the shock velocity, but rather by the lifetime of the source $\Delta t \sim \tau$ [1, 3]. Then, for UHECRs experiencing the effect of multiple shocks, the maximum rigidity is set by the Larmor radius,

$$\mathcal{R}_{L,\max} \sim 10^9 \left(\frac{B}{\mu\text{G}} \right) \left(\frac{R_{\text{SW}}}{\text{kpc}} \right) \text{GV}, \quad (11)$$

with an external constraint set by the energy loss. It is this that we now turn to study.

The final energy after the acceleration process for a fixed species (A, Z) is given by the competition between the superwind acceleration and the possibility that a given nucleus suffers a photodisintegration and becomes a new species (A', Z') after losing one or several nucleons. A nucleus injected into the superwind at a time t_0 has probability $dP = f(t_0, t)dt$ to suffer a photodisintegration in the time in the interval $[t, t + dt]$, where

$$f(t_0, t) = \frac{\mathcal{F}(t_0, t)}{\tau[\mathcal{E}(E_0, t_0, t)]}, \quad (12a)$$

$$\mathcal{F}(t_0, t) = \exp\left(-\int_{t_0}^t \frac{dt'}{\tau(\mathcal{E}(E_0, t_0, t'))}\right), \quad (12b)$$

and $\tau(E)$ is the mean free path for the nucleus at a given energy. The accelerating nucleus will gain energy until it eventually suffers a photodisintegration at a time t distributed following (12a).

The photodisintegration rate depends on the energy density of the ambient radiation field. This is governed by the spatial distribution of photons, including both those from the cosmic microwave background (CMB) and stellar radiation fields. For compact regions near the galaxy core, starbursts exhibit an energy density in their stellar radiation fields which may exceed (or be comparable to) that of the CMB, but at the superwind scale R_{SW} starlight is expected to have a negligible energy density compared to that of the CMB [65, 66]. For our calculations, the contribution from the stellar radiation is unimportant and therefore neglected.

In order to describe the energies that can be achieved through superwind acceleration, we consider the probability $dP = h(E_0, E)dE$ for the photodisintegration to happen at an energy in $[E, E + dE]$. Comparing with (12), the distribution for the final energy is

$$h(E_0, E) = \frac{\mathcal{H}(E, E_0)}{g_{\text{SW}}^{(Z)}\tau(E)}, \quad (13a)$$

$$\mathcal{H}(E_0, E) = \exp\left(-\int_{E_0}^E \frac{dE'}{g_{\text{SW}}^{(Z)}\tau(E')}\right). \quad (13b)$$

The CMB mean free path is described as [4]

$$\tau(E) = \left[\frac{c}{4\pi^2} \left(\frac{m}{\hbar c E} \right)^3 \int_0^\infty \frac{J(\varepsilon)}{e^{\varepsilon/kT'(E)} - 1} d\varepsilon \right]^{-1}, \quad (14)$$

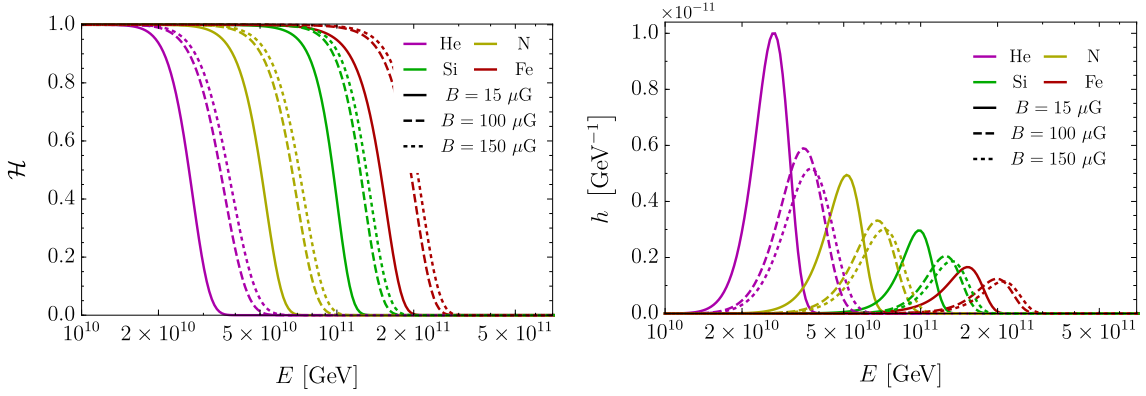


Figure 1: Survival probability (left) and probability density for the energy at which the photodisintegration happens (right), for the four considered nuclei.

where $T'(E) = 2ET/Amc^2$, m is the proton mass, T is the CMB temperature,

$$J(\varepsilon) = \int_0^\varepsilon \varepsilon' \sigma(\varepsilon') d\varepsilon', \quad (15)$$

and where $\sigma(\varepsilon')$ is the cross-section for photo-disintegration by a photon of energy ε' in the rest frame of the nucleus. The \mathcal{H} functions have a decreasing sigmoid shape, as can be seen in Fig. 1. This allows to define a cutoff energy E_c at the point of their largest decrease rate, which corresponds to the peak of the h functions, shown in Fig. 1 as well. This condition reads

$$E_c = \arg \max_{E > E_0} \left(-\frac{d\mathcal{H}(E_0, E)}{dE} \right) = \arg \max_{E > E_0} h(E_0, E). \quad (16)$$

It can be rewritten in terms of the mean free path as

$$1 + g_{\text{sw}}^{(Z)} \frac{d\tau(E)}{dE} \Big|_{E=E_c} = 0, \quad (17)$$

where the independence of E_c on E_0 has been made explicit. The values of the cutoff energy are shown in Fig. 2 for the region of interesting B -strengths. The dispersion around the peak of h suggests that particles of energies above E_c might be achieved at the source. In Fig. 2 we show bands containing the 68% of the probability (i.e. such that $\mathcal{H} \sim 0.16$ and $\mathcal{H} \sim 0.84$), which means that nuclei have around 16% probability of reaching energies above (below) the top (bottom) band. Further calculations show that nitrogen nuclei have a probability of around 7% of reaching energies above $10^{10.95}$ eV and 1% above 10^{11} GeV for $B \sim 150 \mu\text{G}$. The sharp suppression of the probability function with rising energy can accommodate a steeply falling spectrum if silicon-type nuclei are much less abundant than CNO-type nuclei. A detailed study of this function with predictions on nuclear composition to accommodate the observed spectrum on Earth will be presented elsewhere [43].

The relevance of CMB photodisintegration at a certain source depends on the interplay between the lifetime of the source and the mean free path. For short living sources, the

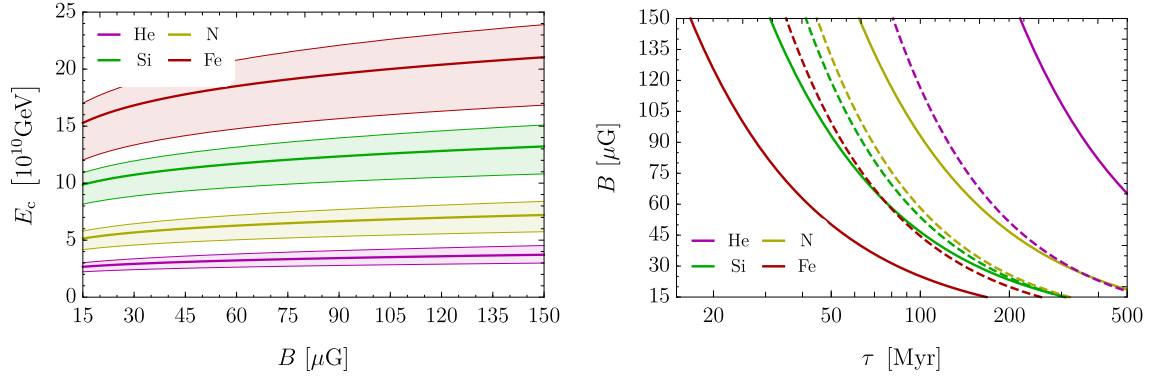


Figure 2: Cutoff energy as a function of the magnetic field for the four considered nuclei (left), and parameter space for the source for a maximum energy of 10^{11} GeV, and limits (dashed) imposed by CMB photodisintegration (right).

energies achieved will not be high enough for the CMB to play a role, and the maximum energy for a certain species will be determined solely due to the lifetime τ and the magnetic field B as in (7). This relation, equivalently written as $B \propto E_{\text{max}}/\tau$, allows to study the parameter space (τ, B) that would allow to reach a certain energy E_{max} . Nevertheless, as the lifetime increases, the available energies will be limited by photodisintegration processes and, given a maximum energy, it will not always be possible to find a pair (τ, B) able to provide such energy, since the CMB interactions would produce a cutoff before that energy is reached. In Fig. 2 we explore this parameter space for a maximum energy of 10^{11} GeV. The continuous lines follow (7), while the dashed lines define the regions (on the right) that are not accessible due to the previous criterion. It can be seen that on average no pair (τ, B) would be able to accelerate helium or nitrogen nuclei above that energy, while the opposite is true for silicon and iron nuclei.

In summary, we have re-examined the acceleration of UHECRs in starburst superwinds endowed with multiple, non-simultaneous, propagating shocks. Particles gain energy when they pass through the shock back and forth after being scattered by the flowing plasma. To calculate the maximum energy we must consider not only particles which are accelerated by a single shock but also particles which undergo many shock encounters, each of which further accelerates the particles. There are two length scales which are important for particle acceleration by multiple shocks: the mean free path for high energy particles and the distance between shocks in the superwind. In our approximation, only the first scale is relevant. We have shown that the particle's maximum energy is set by a balance equation driven by the source lifetime and UHECR interactions with the CMB. This gives specific characteristics for the source emission spectra, providing a new interpretation of the observed suppression in the UHECR spectrum.

Up until now, there were two competing classes of models to explain the observed suppression in the energy spectrum. The competing models are: (i) the GZK cutoff due to the UHECR interaction with the CMB during propagation [14, 15], and (ii) the disappointing model [16, 17] wherein it is postulated that the end-of-stream for cosmic

accelerators $\propto E_{\max}/Z$ is coincidentally near the putative GZK cutoff. More concretely, conventional UHECR source models presuppose that particle acceleration takes place at sites distributed similarly to the matter distribution in the universe, with energy loss processes during propagation leading to the observed flux suppression (GZK cutoff). However, the most recent data seem to indicate that the uppermost end of the cosmic ray energy spectrum is dominated by nucleus-emitting- sources, possibly within the GZK horizon, for which the upper limit of particle acceleration almost coincides with the energy of the GZK suppression. In contrast to conventional expectations, models in category (ii) suggest that the emission of these sources would be characterized by a harder power-law spectrum with the different mass components exhibiting a rigidity-dependent maximum injection energy E_{\max}/Z of a few EeV. Herein, we have introduced an alternative possibility (iii) in which the maximum energy is driven by GZK interactions, but as in (ii) the observed suppression of the energy spectrum mainly stems from the source characteristics rather than being the imprint of particle propagation through the CMB. Note that (iii) is markedly different from (ii) because the maximum energy of acceleration capability of the sources grows linearly in Z , while the energy loss per distance traveled decreases with increasing A .

Class (iii) models have very particular predictions, which can be easily distinguished from those in models of class (ii). For example, if the local distribution of sources dominates the spectrum beyond the suppression, as suggested by anisotropy studies, our new interpretation for the origin of the spectral cutoff explains *naturally* why the maximum energy observed on Earth coincides with that expected from a uniform distribution of sources but with UHECR nuclei propagating over cosmological distances. Moreover, the best fit to the observed spectrum and nuclear composition yields a proton maximum energy $E_{\max}^p = E_{\max}/Z \sim 10^{9.5}$ GeV [28, 29]. This in turn gives a maximum energy for CNO species of $E_{\max}^{\text{CNO}} \sim 10^{10.5}$ GeV, which is below the observed suppression in the energy spectrum [11, 12], and therefore below the energy cutoff in the anisotropy analysis of [31]. Now, the typical values of the deflections of UHECRs crossing the Galaxy are

$$\theta \sim 10^\circ Z \left(\frac{E}{10^{10} \text{ GeV}} \right)^{-1}, \quad (18)$$

and therefore it is challenging to accommodate anisotropy patterns with $Z \gtrsim 8$ nuclei [67]. As we have shown, CNO species can be accelerated in starburst superwinds to the maximum observed energies.

Altogether, this provides a compelling case demonstrating that there is strong evidence favoring UHECRs origin in starburst superwinds.

Note Added

Additional support for the ideas discussed in this paper was presented at the Conference. The Auger Collaboration reported the updated results of searches for anisotropies in the highest energy cosmic rays [68]. With new data the significance of rejecting the isotropic hypothesis from a comparison with a starburst galaxies model has increased to reach

4.5 σ . The IceCube Collaboration reported the updated results of searches for neutrino emission from stacked catalogs of sources [69,70]. A catalog of 110 sources, comprising active galactic nuclei (including blazars), starburst galaxies, and Galactic γ -ray sources was created using γ -ray data to select γ -bright sources that may produce neutrinos. The brightest neutrino source coincides with the brightest catalog source, the starburst galaxy NGC 1068. The significance of the source is 2.9 σ after accounting for trials. In our model, high-energy neutrino emission would be expected from the starburst's core, where cosmic rays of energy $\lesssim E_0$ may experience an effective optical depth to hadronic interactions which is larger than unity. However, the neutrino emission would cutoff somewhat above 10⁷ GeV, as entertained in [71].

Acknowledgments

We thank our colleagues of the Pierre Auger and POEMMA collaborations for some valuable discussions. This work has been supported by the by the U.S. National Science Foundation (NSF Grant PHY-1620661) and the National Aeronautics and Space Administration (NASA Grant 80NSSC18K0464). Any opinions, findings, and conclusions or recommendations expressed in this material are those of the authors and do not necessarily reflect the views of the NSF or NASA.

Appendix

Consider a steady-state planar shock front endowed with a magnetic field. Without loss of generality, the fluid velocity vector \mathbf{u} and the magnetic field vector \mathbf{B} can both be locally broken down into components perpendicular to the shock front (designated by the subscript \perp) and parallel to the shock front (designated by the subscript \parallel). The Rankine-Hugoniot jump conditions for a time-independent magnetohydrodynamic shock are found to be

$$\llbracket \rho u_{\perp} \rrbracket = 0, \quad (19)$$

$$\left\llbracket \rho u_{\perp}^2 + P + \frac{B_{\parallel}^2}{8\pi} \right\rrbracket = 0, \quad (20)$$

$$\left\llbracket \rho u_{\perp} u_{\parallel} - \frac{B_{\perp} B_{\parallel}}{4\pi} \right\rrbracket = 0, \quad (21)$$

$$\left\llbracket \rho u_{\perp} \left(\frac{\gamma}{\gamma-1} \frac{P}{\rho} + \frac{u^2}{2} \right) - \frac{B_{\parallel}}{4\pi} (B_{\perp} u_{\parallel} - B_{\parallel} u_{\perp}) \right\rrbracket = 0, \quad (22)$$

$$\llbracket B_{\perp} u_{\parallel} - B_{\parallel} u_{\perp} \rrbracket = 0, \quad (23)$$

$$\llbracket B_{\perp} \rrbracket = 0. \quad (24)$$

where $\llbracket x \rrbracket \equiv x_1 - x_2$ expresses the jump across the shock, ρ is the mass density and P the thermal pressure, and where quantities measured just upstream of the shock are designated by the subscript "1" and quantities measured just downstream of the shock

are designated by the subscript “2” [72]. Throughout we assume an ideal gas equation of state and so the ratio of specific heats, γ , is considered a constant parameter. It is straightforward to see that if the flow of the gas is perfectly parallel to the field lines so that the shock front is oriented perpendicularly to them (*viz.* $u_{\parallel} = 0$, $u_{\perp} = u$, $B_{\parallel} = 0$, and $B_{\perp} = B$), then the momentum jump condition (20) is the same as in the hydrodynamical case. This makes sense on physical grounds, because within this set up the \mathbf{B} field exerts no net force on the gas, so it is not surprising that the Rankine-Hugoniot jump conditions are hydrodynamic in character [4]. It is also straightforward to see that when $B_{\parallel} \neq 0$ the jump condition for the momentum in the perpendicular direction does depend on the magnetic field, which provides an additional source of pressure. Moreover, the component of the velocity parallel to the shock increases by a factor

$$u_{\parallel 2} - u_{\parallel 1} = \frac{B_{\perp}}{4\pi\rho u_{\perp}}(B_{\parallel 2} - B_{\parallel 1}). \quad (25)$$

For a perpendicular shock, in which $u_{\parallel} = 0$ and the magnetic field is parallel to the shock front (i.e. $B_{\perp} = 0$), we can solve for the density jump ρ_2/ρ_1 in terms of the ratio of the magnetic pressure to the thermal pressure

$$\beta \equiv \frac{B_{\parallel 1}^2}{8\pi P_1}, \quad (26)$$

and the Mach number \mathcal{M} defined as the ratio of the unshocked gas speed to the upstream sound speed. After discarding the trivial solution $\rho_2 = \rho_1$, the Rankine-Hugoniot jump conditions simplify to the quadratic relation

$$2(2-\gamma)\beta\left(\frac{\rho_2}{\rho_1}\right)^2 + \gamma[(\gamma-1)\mathcal{M}^2 + 2(\beta+1)]\left(\frac{\rho_2}{\rho_1}\right) - \gamma(\gamma+1)\mathcal{M}^2 = 0. \quad (27)$$

Therefore, if the magnetic pressure is relatively insignificant (i.e. $\beta \ll \mathcal{M}^2$) the change in density is approximately

$$\frac{\rho_2}{\rho_1} = \zeta \left\{ 1 - \frac{4}{\gamma} \frac{\gamma + \mathcal{M}^2}{[2 + (\gamma - 1)\mathcal{M}^2]^2} \beta \right\} \quad (28)$$

where ζ is the density ratio in the absence of a magnetic field. The presence of a magnetic field thus tends to decrease the density jump from what it would be in the absence of magnetism. As a matter of fact, if we again examine carefully the quadratic equation for ρ_2/ρ_1 , we see that $\rho_2 > \rho_1$ only if

$$\mathcal{M}^2 > 1 + \frac{2}{\gamma}\beta. \quad (29)$$

This implies that the existence of a large magnetic field would allow supersonic motions ($\mathcal{M} > 1$) without the formation of shocks. In closing, we stress once more that the model under consideration herein is that of a parallel shock, for which the energy gain is given by (5) [4, 73].³

³Note that the conventions to identify parallel and perpendicular shocks followed throughout this paper are those in [73] and reversed from those adopted in [4].

References

- [1] L. A. Anchordoqui, G. E. Romero and J. A. Combi, [Heavy nuclei at the end of the cosmic ray spectrum?](#), Phys. Rev. D **60**, 103001 (1999) doi:10.1103/PhysRevD.60.103001 [astro-ph/9903145].
- [2] L. A. Anchordoqui, H. Goldberg and D. F. Torres, [Anisotropy at the end of the cosmic ray spectrum?](#), Phys. Rev. D **67**, 123006 (2003) doi:10.1103/PhysRevD.67.123006 [astro-ph/0209546].
- [3] L. A. Anchordoqui, [Acceleration of ultrahigh-energy cosmic rays in starburst superwinds](#), Phys. Rev. D **97**, no. 6, 063010 (2018) doi:10.1103/PhysRevD.97.063010 [arXiv:1801.07170 [astro-ph.HE]].
- [4] L. A. Anchordoqui, [Ultra-high-energy cosmic rays](#), Phys. Rep. **801**, 1 (2019) doi:10.1016/j.physrep.2019.01.002 [arXiv:1807.09645 [astro-ph.HE]].
- [5] T. M. Heckman and T. A. Thompson, [A brief review of galactic winds](#) arXiv:1701.09062.
- [6] R. L. White, [Synchrotron emission from chaotic stellar winds](#), Astrophys. J. **289**, 698 (1985). doi:10.1086/162933
- [7] J. H. Matthews, A. R. Bell, K. M. Blundell and A. T. Araudo, [Fornax A, Centaurus A, and other radio galaxies as sources of ultrahigh energy cosmic rays](#), Mon. Not. Roy. Astron. Soc. **479**, no. 1, L76 (2018) doi:10.1093/mnrasl/sly099 [arXiv:1805.01902 [astro-ph.HE]].
- [8] P. Schneider, [Diffusive particle acceleration by an ensemble of shock waves](#), Astron. Astrophys. **278**, 315 (1993).
- [9] M. H. Pope and D. B. Melrose, [Diffusive shock acceleration by multiple shock fronts with differing properties](#), Publ. Astron. Soc. Austral. **11**, no. 2, 175 (1994). doi:10.1017/S1323358000019858
- [10] R. U. Abbasi *et al.* [HiRes Collaboration], [First observation of the Greisen-Zatsepin-Kuzmin suppression](#), Phys. Rev. Lett. **100**, 101101 (2008) doi:10.1103/PhysRevLett.100.101101 [astro-ph/0703099].
- [11] J. Abraham *et al.* [Pierre Auger Collaboration], [Observation of the suppression of the flux of cosmic rays above \$4 \times 10^{19}\$ eV](#), Phys. Rev. Lett. **101**, 061101 (2008) doi:10.1103/PhysRevLett.101.061101 [arXiv:0806.4302 [astro-ph]].
- [12] J. Abraham *et al.* [Pierre Auger Collaboration], [Measurement of the energy spectrum of cosmic rays above \$10^{18}\$ eV using the Pierre Auger Observatory](#), Phys. Lett. B **685**, 239 (2010) doi:10.1016/j.physletb.2010.02.013 [arXiv:1002.1975 [astro-ph.HE]].
- [13] T. Abu-Zayyad *et al.* [Telescope Array Collaboration], [The cosmic ray energy spectrum observed with the surface detector of the Telescope Array experiment](#), Astrophys. J. **768**, L1 (2013) doi:10.1088/2041-8205/768/1/L1 [arXiv:1205.5067 [astro-ph.HE]].
- [14] K. Greisen, [End to the cosmic ray spectrum?](#), Phys. Rev. Lett. **16**, 748 (1966) doi:10.1103/PhysRevLett.16.748.
- [15] G. T. Zatsepin and V. A. Kuzmin, [Upper limit of the spectrum of cosmic rays](#), JETP Lett. **4**, 78 (1966) [Pisma Zh. Eksp. Teor. Fiz. **4**, 114 (1966)].
- [16] D. Allard, N. G. Busca, G. Decerprit, A. V. Olinto and E. Parizot, [Implications of the cosmic ray spectrum for the mass composition at the highest energies](#), JCAP **0810**, 033 (2008) doi:10.1088/1475-7516/2008/10/033 [arXiv:0805.4779 [astro-ph]].

- [17] R. Aloisio, V. Berezhinsky and A. Gazizov, **Ultra high energy cosmic rays: The disappointing model**, *Astropart. Phys.* **34**, 620 (2011) doi:10.1016/j.astropartphys.2010.12.008 [arXiv:0907.5194 [astro-ph.HE]].
- [18] R. U. Abbasi *et al.*, **Study of ultrahigh energy cosmic ray composition using Telescope Array’s Middle Drum detector and surface array in hybrid mode**, *Astropart. Phys.* **64**, 49 (2014) doi:10.1016/j.astropartphys.2014.11.004 [arXiv:1408.1726 [astro-ph.HE]].
- [19] R. U. Abbasi *et al.* [TA Collaboration], **Depth of ultra-high energy cosmic ray induced air shower maxima measured by the Telescope Array Black Rock and Long Ridge FADC fluorescence detectors and surface array in hybrid mode**, arXiv:1801.09784 [astro-ph.HE].
- [20] J. Abraham *et al.* [Pierre Auger Collaboration], **Measurement of the depth of maximum of extensive air showers above 10^{18} eV**, *Phys. Rev. Lett.* **104**, 091101 (2010) doi:10.1103/PhysRevLett.104.091101 [arXiv:1002.0699 [astro-ph.HE]].
- [21] A. Aab *et al.* [Pierre Auger Collaboration], **Depth of maximum of air-shower profiles at the Pierre Auger Observatory I: Measurements at energies above $10^{17.8}$ eV**, *Phys. Rev. D* **90**, 122005 (2014) doi:10.1103/PhysRevD.90.122005 [arXiv:1409.4809 [astro-ph.HE]].
- [22] A. Aab *et al.* [Pierre Auger Collaboration], **Depth of maximum of air-shower profiles at the Pierre Auger Observatory II: Composition implications**, *Phys. Rev. D* **90**, 122006 (2014) doi:10.1103/PhysRevD.90.122006 [arXiv:1409.5083 [astro-ph.HE]].
- [23] A. Aab *et al.* [Pierre Auger Collaboration], **Inferences on mass composition and tests of hadronic interactions from 0.3 to 100 EeV using the water-Cherenkov detectors of the Pierre Auger Observatory**, *Phys. Rev. D* **96**, 122003 (2017) doi:10.1103/PhysRevD.96.122003 [arXiv:1710.07249 [astro-ph.HE]].
- [24] A. Aab *et al.* [Pierre Auger Collaboration], **Evidence for a mixed mass composition at the “ankle” in the cosmic-ray spectrum**, *Phys. Lett. B* **762**, 288 (2016) doi:10.1016/j.physletb.2016.09.039 [arXiv:1609.08567 [astro-ph.HE]].
- [25] R. Abbasi *et al.* [Pierre Auger and TA Collaborations], **Report of the working group on the composition of ultrahigh energy cosmic rays**, *JPS Conf. Proc.* **9**, 010016 (2016) doi:10.7566/JPSCP.9.010016 [arXiv:1503.07540].
- [26] W. Hanlon *et al.*, **Report of the working group on the mass composition of ultrahigh energy cosmic rays**, *JPS Conf. Proc.* **19**, 011013 (2018). doi:10.7566/JPSCP.19.011013
- [27] A. A. Watson, **The highest energy cosmic rays: the past, the present and the future**, arXiv:1901.06676 [astro-ph.IM].
- [28] A. Aab *et al.* [Pierre Auger Collaboration], **Combined fit of spectrum and composition data as measured by the Pierre Auger Observatory**, *JCAP* **1704**, no. 04, 038 (2017) Erratum: [*JCAP* **1803**, no. 03, E02 (2018)] doi:10.1088/1475-7516/2018/03/E02, 10.1088/1475-7516/2017/04/038 [arXiv:1612.07155 [astro-ph.HE]].
- [29] M. Unger, G. R. Farrar and L. A. Anchordoqui, **Origin of the ankle in the ultrahigh energy cosmic ray spectrum, and of the extragalactic protons below it**, *Phys. Rev. D* **92**, 123001 (2015) doi:10.1103/PhysRevD.92.123001 [arXiv:1505.02153 [astro-ph.HE]].
- [30] A. M. Taylor, M. Ahlers and D. Hooper, **Indications of negative evolution for the sources of the highest energy cosmic rays**, *Phys. Rev. D* **92**, no. 6, 063011 (2015) doi:10.1103/PhysRevD.92.063011 [arXiv:1505.06090 [astro-ph.HE]].

- [31] A. Aab *et al.* [Pierre Auger Collaboration], **An Indication of anisotropy in arrival directions of ultra-high-energy cosmic rays through comparison to the flux pattern of extragalactic gamma-ray sources**, *Astrophys. J.* **853**, L29 (2018) [arXiv:1801.06160 [astro-ph.HE]].
- [32] R. U. Abbasi *et al.* [TA Collaboration], **Search for correlations between arrival directions of ultrahigh-energy cosmic rays detected by the Telescope Array experiment and a flux pattern from nearby starburst galaxies**, *Astrophys. J.* **867**, L27 (2018) [arXiv:1809.01573 [astro-ph.HE]].
- [33] R. U. Abbasi *et al.* [TA Collaboration], **Indications of intermediate-scale anisotropy of cosmic rays with energy greater than 57 EeV in the Northern sky measured with the surface detector of the Telescope Array experiment**, *Astrophys. J.* **790**, L21 (2014) [arXiv:1404.5890 [astro-ph.HE]].
- [34] K. Kawata *et al.* [TA Collaboration], **Ultra-high-energy cosmic-ray hotspot observed with the Telescope Array surface detectors**, *PoS ICRC 2015*, 276 (2016).
- [35] H. N. He, A. Kusenko, S. Nagataki, B. B. Zhang, R. Z. Yang and Y. Z. Fan, **Monte Carlo Bayesian search for the plausible source of the Telescope Array hotspot**, *Phys. Rev. D* **93**, 043011 (2016) doi:10.1103/PhysRevD.93.043011 [arXiv:1411.5273 [astro-ph.HE]].
- [36] D. N. Pfeffer, E. D. Kovetz and M. Kamionkowski, **Ultrahigh-energy cosmic ray hotspots from tidal disruption events**, *Mon. Not. Roy. Astron. Soc.* **466**, no. 3, 2922 (2017) doi:10.1093/mnras/stw3337 [arXiv:1512.04959 [astro-ph.HE]].
- [37] J. Kim, D. Ryu, H. Kang, S. Kim and S. C. Rey, **Filaments of galaxies as a clue to the origin of ultra-high-energy cosmic rays**, *Science Advances* **5**, eaau8227 (2019) doi:10.1126/sciadv.aau8227 [arXiv:1901.00627 [astro-ph.HE]].
- [38] N. Globus, D. Allard, E. Parizot, C. Lachaud and T. Piran, **Can we reconcile the TA excess and hotspot with Auger observations?**, *Astrophys. J.* **836**, no. 2, 163 (2017) doi:10.3847/1538-4357/836/2/163 [arXiv:1610.05319 [astro-ph.HE]].
- [39] B. T. Zhang, K. Murase, S. S. Kimura, S. Horiuchi and P. Meszaros, **Low-luminosity gamma-ray bursts as the sources of ultrahigh-energy cosmic ray nuclei**, *Phys. Rev. D* **97**, no. 8, 083010 (2018) doi:10.1103/PhysRevD.97.083010 [arXiv:1712.09984 [astro-ph.HE]].
- [40] X. Y. Wang, S. Razzaque, P. Meszaros and Z. G. Dai, **High-energy cosmic rays and neutrinos from semi-relativistic hypernovae**, *Phys. Rev. D* **76**, 083009 (2007) doi:10.1103/PhysRevD.76.083009 [arXiv:0705.0027 [astro-ph]].
- [41] P. O. Lagage and C. J. Cesarsky, **The maximum energy of cosmic rays accelerated by supernova shocks**, *Astron. Astrophys.* **125**, 249 (1983).
- [42] T. K. Gaisser, *Cosmic rays and particle physics*, (Cambridge University Press, 1990) ISBN 0-521-32667-2.
- [43] J. F. Soriano and L. A. Anchordoqui, in preparation.
- [44] G. E. Romero, A. L. Müller and M. Roth, **Particle acceleration in the superwinds of starburst galaxies**, *Astron. Astrophys.* **616**, A57 (2018) doi:10.1051/0004-6361/201832666 [arXiv:1801.06483 [astro-ph.HE]].
- [45] B. C. Lacki, **From 10K to 10 TK: Insights on the interaction between cosmic rays and gas in starbursts**, *Astrophys. Space Sci. Proc.* **34**, 411 (2013) doi:10.1007/978-3-642-35410-6_29 [arXiv:1308.5241 [astro-ph.HE]].

- [46] A. M. Hillas, *The origin of ultrahigh-energy cosmic rays*, *Ann. Rev. Astron. Astrophys.* **22**, 425 (1984). doi:10.1146/annurev.aa.22.090184.002233
- [47] T. M. Heckman, L. Armus and G. K. Miley, *On the nature and implications of starburst-driven galactic superwinds*, *Astrophys. J. Suppl.* **74**, 833 (1990). doi:10.1086/191522
- [48] T. A. Thompson, E. Quataert, E. Waxman, N. Murray and C. L. Martin, *Magnetic fields in starburst galaxies and the origin of the fir-radio correlation*, *Astrophys. J.* **645**, 186 (2006) [astro-ph/0601626].
- [49] J. D. Bregman, P. Temi, and D. Rank, *Direct measurement of the supernova rate in starburst galaxies*, *Astron. Astrophys.* **355**, 525 (2000).
- [50] B. Adebahr, M. Krause, U. Klein, M. Wezgowiec, D. J. Bomans and R.-J. Dettmar, *M82 - A radio continuum and polarisation study I: Data reduction and cosmic ray propagation*, *Astron. Astrophys.* **555**, A23 (2013) doi:10.1051/0004-6361/201220226 [arXiv:1209.5552 [astro-ph.GA]].
- [51] B. Adebahr, M. Krause, U. Klein, G. Heald, and R.-J. Dettmar, *M82 - A radio continuum and polarisation study II: Polarization and rotation measures*, *Astron. Astrophys.* **608**, A29 (2017) doi:10.1051/0004-6361/201629616 [arXiv:1710.04050 [astro-ph.GA]].
- [52] R. Beck, C. L. Carilli, M. A. Holdaway, and U. Klein, *Multifrequency observations of the radio continuum emission from NGC 253 I: Magnetic fields and rotation measures in the bar and halo*, *Astron. Astrophys.* **292**, 409 (1994).
- [53] V. Heesen, R. Beck, M. Krause and R.-J. Dettmar, *Cosmic rays and the magnetic field in the nearby starburst galaxy NGC 253 I: The distribution and transport of cosmic rays*, *Astron. Astrophys.* **494**, 563 (2009) doi:10.1051/0004-6361:200810543 [arXiv:0812.0346 [astro-ph]].
- [54] V. Heesen, M. Krause, R. Beck and R. J. Dettmar, *Cosmic rays and the magnetic field in the nearby starburst galaxy NGC 253 II: The magnetic field structure*, *Astron. Astrophys.* **506**, 1123 (2009) doi:10.1051/0004-6361/200911698 [arXiv:0908.2985 [astro-ph.CO]].
- [55] V. Heesen, R. Beck, M. Krause and R. J. Dettmar, *Cosmic rays and the magnetic field in the nearby starburst galaxy NGC 253 III: Helical magnetic fields in the nuclear outflow*, *Astron. Astrophys.* **535**, A79 (2011) doi:10.1051/0004-6361/201117618 [arXiv:1109.0255 [astro-ph.CO]].
- [56] M. Krause, *Magnetic fields and halos in spiral galaxies*, arXiv:1401.1317 [astro-ph.GA].
- [57] B. C. Lacki and R. Beck, *The equipartition magnetic field formula in starburst galaxies: Accounting for pionic secondaries and strong energy losses*, *Mon. Not. Roy. Astron. Soc.* **430**, 3171 (2013) doi:10.1093/mnras/stt122 [arXiv:1301.5391 [astro-ph.CO]].
- [58] D. F. Torres, *Theoretical modelling of the diffuse emission of gamma-rays from extreme regions of star formation: The Case of Arp 220*, *Astrophys. J.* **617**, 966 (2004) doi:10.1086/425415 [astro-ph/0407240].
- [59] J. McBride, T. Robishaw, C. Heiles, G. C. Bower, and A. P. Sarma, *Parsec-scale magnetic fields in Arp 220*, *Mon. Not. Roy. Astron. Soc.* **447**, 1103 (2015) doi:10.1093/mnras/stu2489 [arXiv:1411.7407].
- [60] D. F. Torres, A. Cillis, B. Lacki and Y. Rephaeli, *Building up the spectrum of cosmic-rays in star-forming regions*, *Mon. Not. Roy. Astron. Soc.* **423**, 822 (2012) doi:10.1111/j.1365-2966.2012.20920.x [arXiv:1203.2798 [astro-ph.HE]].

- [61] T. A. D. Paglione and R. D. Abrahams, **Properties of nearby starburst galaxies based on their diffuse gamma-ray emission**, *Astrophys. J.* **755**, 106 (2012) doi:10.1088/0004-637X/755/2/106 [arXiv:1206.3530 [astro-ph.HE]].
- [62] E. Domingo-Santamaria and D. F. Torres, **High energy gamma-ray emission from the starburst nucleus of NGC 253**, *Astron. Astrophys.* **444**, 403 (2005) doi:10.1051/0004-6361:20053613 [astro-ph/0506240].
- [63] E. de Cea del Pozo, D. F. Torres and A. Y. R. Marrero, **Multi-messenger model for the starburst galaxy M82**, *Astrophys. J.* **698**, 1054 (2009) doi:10.1088/0004-637X/698/2/1054 [arXiv:0901.2688 [astro-ph.GA]].
- [64] B. C. Lacki, **Sturm und drang: Supernova-driven turbulence, magnetic fields, and cosmic rays in the chaotic starburst interstellar medium**, arXiv:1308.5232 [astro-ph.CO].
- [65] L. A. Anchordoqui, D. Hooper, S. Sarkar and A. M. Taylor, **High-energy neutrinos from astrophysical accelerators of cosmic ray nuclei**, *Astropart. Phys.* **29**, 1 (2008) doi:10.1016/j.astropartphys.2007.10.006 [astro-ph/0703001].
- [66] E. R. Owen, K. Wu, X. Jin, P. Surajbali and N. Kataoka, **Starburst and post-starburst high-redshift protogalaxies: The feedback impact of high energy cosmic rays**, doi:10.1051/0004-6361/201834350 arXiv:1905.00338 [astro-ph.GA].
- [67] R. C. dos Anjos *et al.*, **Ultrahigh-energy cosmic ray composition from the distribution of arrival directions**, *Phys. Rev. D* **98**, no. 12, 123018 (2018) doi:10.1103/PhysRevD.98.123018 [arXiv:1810.04251 [astro-ph.HE]].
- [68] L. Caccianiga *et al.* [Pierre Auger Collaboration], **Anisotropies of the highest energy cosmic-ray events recorded by the Pierre Auger Observatory in 15 years of operation, in these proceedings**.
- [69] T. Carver [IceCube Collaboration], **Ten years of all-sky neutrino point-source searches**, arXiv:1908.05993 [astro-ph.HE].
- [70] M. G. Aartsen *et al.* [IceCube Collaboration], **The IceCube neutrino observatory: Contributions to the 36th International Cosmic Ray Conference (ICRC2019)**, arXiv:1907.11699 [astro-ph.HE].
- [71] A. Loeb and E. Waxman, **The cumulative background of high energy neutrinos from starburst galaxies**, *JCAP* **0605**, 003 (2006) doi:10.1088/1475-7516/2006/05/003 [astro-ph/0601695].
- [72] F. de Hoffmann and E. Teller, **Magneto-hydrodynamic shocks**, *Phys. Rev.* **80**, 692 (1950). doi:10.1103/PhysRev.80.692
- [73] R. J. Protheroe, **Acceleration and interaction of ultrahigh-energy cosmic rays**, [astro-ph/9812055].